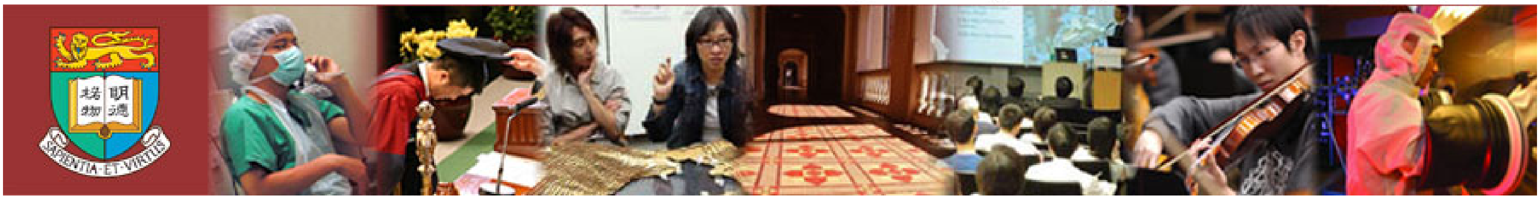

Title	Asymmetry dependence of reduction factors from single-nucleon knockout of ³⁰Ne at 230 MeV/nucleon
Author(s)	Lee, HCJ; Liu, H; Doornenbal, P; Kimura, M; Minomo, K; Ogata, K; Utsuno, Y; Aoi, N; Li, K; Matsushita, M; Scheit, H; Steppenbeck, D; Takeuchi, S; Wang, H; Baba, H; Ideguchi, E; Kobayashi, N; Kondo, Y; Michimasa, S; Motobayashi, T; Sakurai, H; Takechi, M; Togano, Y
Citation	Progress of Theoretical and Experimental Physics, 2016, v. 2016 n. 8, p. 083D01:1-7
Issued Date	2016
URL	http://hdl.handle.net/10722/231234
Rights	This work is licensed under a Creative Commons Attribution-NonCommercial-NoDerivatives 4.0 International License.

PTEP

Prog. Theor. Exp. Phys. **2016**, 083D01 (7 pages)
DOI: 10.1093/ptep/ptw096

Asymmetry dependence of reduction factors from single-nucleon knockout of ^{30}Ne at ∼ 230 MeV/nucleon

J. Lee[1,2,*], H. Liu[1,3], P. Doornenbal[1], M. Kimura[4], K. Minomo[5,6], K. Ogata[6], Y. Utsuno[7], N. Aoi[1], K. Li[1,3], M. Matsushita[1], H. Scheit[1], D. Steppenbeck[1], S. Takeuchi[1], H. Wang[1,3], H. Baba[1], E. Ideguchi[8], N. Kobayashi[9], Y. Kondo[9], S. Michimasa[8], T. Motobayashi[1,10], H. Sakurai[1], M. Takechi[1], and Y. Togano[1]

[1] *RIKEN Nishina Center, Wako, Saitama 351-0198, Japan*
[2] *Department of Physics, The University of Hong Kong, Hong Kong, China*
[3] *State Key Laboratory of Nuclear Physics and Technology, Peking University, Beijing 100871, China*
[4] *Department of Physics, Hokkaido University, Sapporo 060-0810, Japan*
[5] *Department of Physics, Kyushu University, Fukuoka 812-8581, Japan*
[6] *Research Center for Nuclear Physics, Osaka University, Ibaraki 567-0047, Japan*
[7] *Japan Atomic Energy Agency, Tokai, Ibaraki 319-1195, Japan*
[8] *Center for Nuclear Study, University of Tokyo, Wako, Saitama, 351-0198, Japan*
[9] *Department of Physics, Tokyo Institute of Technology, Meguro, Tokyo 152-8551, Japan*
[10] *Department of Physics, Rikkyo University, Toshima, Tokyo 172-8501, Japan*
*E-mail: jleehc@hku.hk

Received November 13, 2015; Revised May 25, 2016; Accepted May 30, 2016; Published August 8, 2016

The single-neutron and -proton removal reactions of ^{30}Ne with large separation-energy asymmetry $|\Delta S| = |S_n - S_p|$ at incident energies of about 230 MeV/nucleon are measured. In the case of the deeply bound nucleon removal data, a large disagreement is obtained from the theoretical cross sections calculated using the eikonal reaction theory, with nuclear structure inputs from the many-body shell-model theory and the antisymmetrized molecular dynamics theory, respectively. Such a discrepancy is consistent with the systematics observed from the knockout reactions at incident energies ∼ 100 MeV/nucleon.

Subject Index D20, D21, D27

1. Introduction

A full understanding of nuclear properties requires an accurate knowledge of correlations between the nucleons. The correlations spread the contributions from single-particle orbits and result in a reduction of the nucleon occupancies relative to the independent-particle-model (IPM) values [1]. Assuming that the reaction mechanism description is well under control, deviations from unity of the ratio $R_s = \sigma(\text{expt})/\sigma(\text{theory})$ indicate the onset of correlation strength missing in the structure theories.

A constant quenching (30–40%) of the valence proton spectroscopic strengths was observed in $(e, e'p)$ reaction studies for nuclei near a closed shell compared to the IPM values [2]. Such suppression of the spectroscopic factors (SF) clearly indicates an insufficient treatment of nucleon–nucleon correlations in the present shell models for nuclei near stability [1–3]. It is imperative to understand how these correlations change in nuclei away from stability and to what extent the theories have predictive power.

The ^{9}Be and ^{12}C target-induced one-nucleon ($1N$) knockout measurements at energies below 90 MeV/nucleon suggest a strong asymmetry dependence of the reduction factor R_s [4]. The results indicate a strong dependence of R_s on the asymmetry of the Fermi surfaces in each nucleus, which is characterized by ΔS, the difference between the neutron and proton separation energies ($\Delta S = S_n - S_p$ for neutron SF and $\Delta S = S_p - S_n$ for proton SF). Such established systematics could suggest that deeply bound nucleons experience additional correlations, which are not taken into account in effective interaction theories [4], although a deficiency in the reaction mechanism treatment dependent on the removed-nucleon binding energy cannot be excluded.

In contrast, the one-neutron transfer reactions on argon isotopes with a large span of asymmetry at NSCL suggest a weak dependence of correlations on the neutron–proton asymmetry [5,6]. This large disagreement for deeply bound systems has not been explained so far and is inconsistent with results from systematic studies of transfer reactions [7–10] and other theoretical calculations such as dispersive-optical-model (DOM) studies [11,12], the modern Green's function calculations [13], and the microscopic coupled-cluster calculations coupling-to-continuum [14]. More recently, results from an experiment at GANIL aiming to study $^{14}\mathrm{O}(d,t)$ [15] indicated that no strong reduction is observed from the transfer reaction, even for nuclei with a large asymmetry $\Delta S = |S_n - S_p| = 18.6$ MeV ($S_N = 23.2$ MeV; $S_p = 4.63$ MeV).

The corresponding stripping measurement of ^{14}O at 60 MeV/nucleon has been performed at NSCL and revealed a strong reduction of the one-neutron removal cross section compared to shell-model+eikonal predictions [16]. The parallel momentum distributions obtained from this work exhibit a large tail at low momentum, originating in part from dissipative processes during the core–target interaction, and an abrupt cutoff at high momentum due to the incident energy being comparable to the initial neutron separation energy, keeping some part of the flux from being visible in the final state as a result [16].

Being rooted in the eikonal and sudden approximations, the nucleon knockout model is formulated for reactions at energies of about 80 MeV/nucleon or higher [17,18]. At such high energies, the nucleon removal mechanism is expected to be surface dominant, which allows the survival of the core nucleus (heavy residue) and eliminates the need to specify the motion of fast nucleons in the nuclear interior [17,18]. This simple picture of a reaction mechanism with a nucleon being removed from a frozen nucleus, however, has long been questioned [19]. It is essential to test the energy dependence of the reaction mechanism and modeling. Existing published data on one-nucleon removal of deeply bound nuclei were obtained at energies below 120 MeV/nucleon [4,20]. It is possible that the beam energies are not sufficiently high for the approximations employed in the eikonal theories to be valid, in particular the eikonal approximation to the scattering waves and adiabatic approximation for the projectile. Knockout reaction data on deeply bound nucleons at higher energies are missing and therefore desirable for energy dependence studies of reaction mechanisms.

In this work, we perform the first deeply bound nucleon removal ($|\Delta S| > 20$ MeV) at an energy above 200 MeV/nucleon. The reaction used is $^{12}\mathrm{C}(^{30}\mathrm{Ne}, ^{29}\mathrm{F})\mathrm{X}$ at 230 MeV/nucleon. The ^{30}Ne nucleus has a large difference in individual nucleon separation energies of 20.5 MeV (S_p = 23.9 MeV and S_N = 3.4 MeV), similar to cases where strong discrepancies between experimental and theoretical results have been observed. To achieve a systematic study covering both extremes of the isospin asymmetry, the cross sections of the loosely bound neutron in ^{30}Ne are also measured with the ^{12}C(^{30}Ne, ^{29}Ne)X reaction.

2. Experiments

The experiment was performed at the Radioactive Isotope Beam Factory [21], operated by the RIKEN Nishina Center, and CNS, University of Tokyo. The superconducting ring cyclotron supplied a ^{48}Ca primary beam at 345 MeV/nucleon with the beam intensity $\sim$ 75 pnA. The ^{30}Ne secondary beam, produced by projectile fragmentation at a 15 mm thick rotating Be target, had an intensity of 440 particles per second and a momentum spread ($\Delta P/P$) of $\pm 3\%$. The ^{30}Ne beam was identified event-by-event according to the magnetic rigidity ($B\rho$), time of flight (TOF), and energy loss (ΔE) obtained by the standard detectors of the fragment separator BigRIPS [21,22]. The secondary beam bombarded a C target of 2.54 g/cm^2 thickness with a mid-target energy of 228 MeV/nucleon. After the reactions, the ^{29}F and ^{29}Ne residues produced were identified by their $B\rho$, TOF, and ΔE measured with the ZeroDegree Spectrometer [22]. In addition, the de-excitation gammas from these reaction residues were measured by the gamma-ray detector array DALI2 [23], which was composed of 186 NaI (Tl) scintillator crystals and surrounded the reaction target. The details of the experimental setup, particle identification of the beam and reaction residues, analytical procedures, and spectra can be found in P. Doornenbal et al. and H. Liu et al. (manuscripts in preparation).

For the ^{12}C(^{30}Ne, ^{29}F)X and ^{12}C(^{30}Ne, ^{29}Ne)X reactions, the measured inclusive cross sections were 5.8(3) mb and 62(2) mb, respectively. The exclusive-to-final-state cross sections were also measured and ground-state cross sections subsequently deduced (P. Doornenbal et al. and H. Liu et al., manuscripts in preparation). It should be noted that, because of a limit due to the detectors' thresholds, there was a possibility that a measured cross section with no coincidence with gamma-rays contained contributions from low-lying excited states of the residual nucleus below about 200 keV. Considering the complexity in the structure of ^{30}Ne and the possible low-lying states below 200 keV in ^{29}Ne and ^{29}F, we therefore focus on the residual bound-state inclusive cross section in the present work. The overall shell-model strengths and reaction yields are compared with the measured cross sections, which are presented as $R_s = \sigma(\text{expt})/\sigma(\text{theory})$.

3. Theoretical analysis and discussion

The structures of ^{30}Ne, ^{29}Ne, and ^{29}F are calculated using two different approaches: shell-model (SM) calculations in the *sd–pf* model space with the SDPF-M effective interaction [24], and anti-symmetrized molecular dynamics (AMD). The AMD calculation with the Gogny D1S interaction [25] was carried out in the same way as that for other Ne and Mg isotopes [26–28]. The results of the structural information on the ground state of ^{30}Ne in terms of the ^{29}F plus p and ^{29}Ne plus n configurations are summarized in Table 1; the spectroscopic factor and the excitation energy of the core nucleus, ^{29}F or ^{29}Ne, for each configuration are shown.

For ^{29}F, both models suggest that the ground state (g.s.) spin-parity is $5/2^+$. The larger spectroscopic factor obtained by the SM (1.485) than that by AMD (0.86) is due to the difference in the ^{29}F($5/2^+$) structure. The ground state of ^{30}Ne is dominated by intruder configurations in both the SM and AMD calculations, whereas that of ^{29}F contains larger $0p$–$0h$ components in AMD than in SM. This leads to the difference in overlap probability when a proton is removed from ^{30}Ne.

For ^{29}Ne, the SM and AMD give different values of the g.s. spin-parity. The situation is complicated by several predicted low-lying excited states below 1 MeV. Fortunately, however, a β-decay experiment has put strong constraints on the possible spin-parity values [29]. The β decay of ^{29}Ne

Table 1. Spectroscopic factors S predicted by the SM and AMD. The values in parentheses represent the excitation energies of ^{29}F or ^{29}Ne.

^{30}Ne configurations	S	
	SM	AMD
^{29}F$(5/2^+_1) \otimes p(d_{5/2})$	1.485 (0 MeV)	0.86 (0 MeV)
^{29}F$(1/2^+_1) \otimes p(s_{1/2})$	0.257 (0.785 MeV)	0.39 (1.91 MeV)
^{29}F$(3/2^+_1) \otimes p(d_{3/2})$	0.120 (2.305 MeV)	0.10 (1.80 MeV)
^{29}F$(3/2^+_2) \otimes p(d_{3/2})$	0.017 (3.481 MeV)	0.00 (2.10 MeV)
^{29}Ne$(3/2^+_1) \otimes n(d_{3/2})$	1.173 (0 MeV)	1.33 (0.14 MeV)
^{29}Ne$(3/2^+_2) \otimes n(d_{3/2})$	0.093 (1.365 MeV)	0.12 (0.97 MeV)
^{29}Ne$(3/2^-_1) \otimes n(p_{3/2})$	0.512 (0.073 MeV)	0.79 (0.61 MeV)
^{29}Ne$(3/2^-_2) \otimes n(p_{3/2})$	0.128 (0.656 MeV)	0.12 (0.99 MeV)
^{29}Ne$(7/2^-_1) \otimes n(f_{7/2})$	1.778 (0.125 MeV)	0.87 (0.79 MeV)
^{29}Ne$(1/2^+_1) \otimes n(s_{1/2})$	0.278 (0.563 MeV)	1.06 (0 MeV)
^{29}Ne$(1/2^+_2) \otimes n(s_{1/2})$	1.165 (2.291 MeV)	0.11 (1.07 MeV)
^{29}Ne$(5/2^+_1) \otimes n(d_{5/2})$	0.012 (1.460 MeV)	0.12 (0.91 MeV)

directly feeds the 72 keV, 1249 keV, and 1588 keV levels in ^{29}Na through a Gamow–Teller transition. These levels are considered to be positive-parity states because low-lying negative-parity states in ^{29}Na, which are dominated by odd-particle, odd-hole excitations across the $N = 20$ gap, should be located rather high ($E_x \gtrsim 3$ MeV) due to strong pairing correlations in neutrons. It is thus quite unlikely that the parent nucleus ^{29}Ne has a negative-parity ground state. In addition, the 72 keV state in ^{29}Na is reasonably assigned as a $5/2^+$ state from the measured $B(E_2;\text{g.s.} \to 72\text{ keV})$ value [30] and comparison to shell-model calculations using the SDPF-M interaction. Taking those experimental data into consideration, the ground state of ^{29}Ne is either $3/2^+$, $5/2^+$, or $7/2^+$. As shown in Table 1, the $5/2^+$ state is located at 1.485 MeV (SM) or 0.86 MeV (AMD). In both models, the $7/2^+$ state has even higher energies.

In the AMD calculation, a $1/2^+$ g.s. of ^{29}Ne is suggested and the $3/2^+$ state is located at 140 keV. These states belong to a rotational band with $K = 1/2$, and the order of these two levels depends rather strongly on the decoupling parameter, as discussed, e.g., in the case of ^{33}Mg [31–33]. Note that, in Ref. [34], the reaction cross section σ_R of ^{29}Ne was calculated with the AMD wave function of the $1/2^+$ g.s., which agreed well with the experimental data [35]. It is confirmed, however, that the observed σ_R of ^{29}Ne is also reproduced well when the $3/2^+$ wave function of ^{29}Ne is taken in the calculation. Thus, a $3/2^+$ assignment is not excluded. On the other hand, the one-neutron removal measurement from ^{29}Ne suggests that the ground state of ^{29}Ne has a spin-parity of $3/2^-$ [36], in contrast to the β-decay experiment in ^{29}Ne [29], which indicates the positive-parity ground state based on direct beta feeding to the $5/2^+$ state (at 72 keV) in ^{29}Na. A possible scenario to account for this contradiction is the existence of a very low-lying isomeric $3/2^-$ state in ^{29}Ne (less than 100 keV). In our analysis in this paper, we therefore concentrate on inclusive cross sections and include both the $3/2^-$ and $3/2^+$ levels for ^{29}Ne.

The one-nucleon removal cross sections σ_{-1N} (N is p or n) are calculated using the eikonal reaction theory (ERT) [37,38], i.e., an extension of the continuum-discretized coupled-channel method (CDCC) [39] applicable to inclusive observables. We take three-body models, (^{29}Ne+n)+^{12}C for one-neutron removal and (^{29}F+p)+^{12}C for one-proton removal. The core–target (nucleon–target) potential is obtained by the double (single) folding model with the Melbourne g-matrix interaction.

Table 2. One-nucleon removal cross sections with different radial parameter (r_0) values.

Calc. configurations	σ_{-1N} with $S = 1$ (mb)		
	r_0 = 1.25 fm	r_0 = 1.375 fm	r_0 = 1.136 fm
^{29}Ne($3/2^+_1$) $\bigotimes$ $d_{3/2}$	22.3	26.0 (+16.6%)	19.3 (−13.5%)
Inclusive (shell model)	94.0	108.6 (+15.5%)	82.0 (−12.8%)
Inclusive (AMD)	112.9	127.8(+13.2%)	100.5(−11.0%)
^{29}F($5/2^+_1$) $\bigotimes$ $d_{5/2}$	11.1	13.4 (+20.7%)	9.4 (−15.3%)
Inclusive (shell model)	19.6	23.5 (+19.9%)	16.7 (−14.8%)
Inclusive (AMD)	9.5	11.5(+21.1%)	8.1(−14.7%)

In the folding calculation, ^{29}Ne($1/2^+$) and ^{29}F($5/2^+$) densities obtained by AMD and the phenomenological ^{12}C density are used. We adopt a central Woods–Saxon potential with a radial (diffuseness) parameter of 1.25 fm (0.65 fm) to generate p-^{29}F and n-^{29}Ne wave functions. To estimate the uncertainties of the present model, we change the value of r_0 by 10%, which leads to 10–20% variation in the calculated cross sections, as shown in Table 2. The depth of the potential is determined to reproduce the experimental nucleon separation energy S_N. In the CDCC calculation, we neglect the intrinsic spin of each particle. The model space of CDCC is the same as in Ref. [37], which gives a good convergence of σ_{-1N}. We calculate σ_{-1N} for each configuration, as shown in Table 1. Then the σ_{-1N} are multiplied by the spectroscopic factor predicted by the SM or AMD and the result is compared with the experimental data.

The calculated σ_{-1p} for the ^{12}C(^{30}Ne, ^{29}F)X reaction are shown in Table 3. Assuming that all bound states in ^{29}F contributing to the one-nucleon strength are calculated, inclusive cross sections of 19.6 mb and 9.5 mb (considering states below 1.44 MeV) are obtained with the spectroscopic factors of ^{29}F given by either the SM or AMD, respectively. The reduction factor R_s in the present case is 0.30 (SM) and 0.61 (AMD).

The SM result significantly overshoots the experimental value of 5.8(3) mb. This feature is consistent with that reported in previous studies on deeply bound nucleon removal around 100 MeV/nucleon by Tostevin and Gade [40]. On the other hand, as shown in Table 3, the calculated inclusive cross sections of the ^{12}C(^{30}Ne, ^{29}Ne)X reaction with the spectroscopic factor obtained by the SM (AMD) are 94.0 mb (112.9 mb), resulting in R_s of 0.66 (0.55). The results are significantly smaller than the established systematics of R_s, which is close to unity for loosely bound nucleon removal [40]. This $R_s \sim 1$ could be understood as the loosely bound nucleon not being effectively influenced by the nucleon–nucleon correlations beyond those described by the shell model. Such deviation of the present result from the reported systematics in Ref. [40] might therefore imply the incomplete description of SM and AMD to the complex structure of ^{30}Ne and ^{29}Ne.

^{30}Ne is a deformed nucleus described as a mixture of many shell-model configurations, resulting in additional uncertainties in investigating the reaction model. In addition, there is no measurement of the ^{12}C(^{30}Ne, ^{29}F)X reaction at lower energy to compare with the present results at ∼ 230 MeV/u. To study the reaction energy dependence in the reaction model with a well-controlled structure model dependence, future measurements of ^{12}C(^{30}Ne, ^{29}F)X at ∼ 100 MeV/u are needed. If the R_s extracted at both low- and high-energies are consistently small, it suggests that a reexamination of the reaction theory description of knockout reactions, including the reaction mechanisms and the input parameters used in these analyses, may be needed.

Table 3. The calculated one-proton and one-neutron removal cross sections σ_{-1N} with the spectroscopic factors predicted by the SM and AMD. The inclusive cross sections are the sum of contributions by the states below the threshold for particle emission. 1.44 MeV is cited from Ref. [41] and 0.963 MeV is obtained by the atomic mass evaluation in 2012 [42].

^{30}Ne configurations	σ_{-1N} (mb)	
	SM	AMD
^{29}F$(5/2^+_1) \otimes p(d_{5/2})$	16.5	9.5
^{29}F$(1/2^+_1) \otimes p(s_{1/2})$	3.1	4.8
^{29}F$(3/2^+_1) \otimes p(d_{3/2})$	1.3	1.1
^{29}F$(3/2^+_2) \otimes p(d_{3/2})$	0.2	0.0
Inclusive (below 1.44 MeV)	19.6	9.5
^{29}Ne$(3/2^+_1) \otimes n(d_{3/2})$	26.2	29.7
^{29}Ne$(3/2^+_2) \otimes n(d_{3/2})$	2.1	2.7
^{29}Ne$(3/2^-_1) \otimes n(p_{3/2})$	17.5	27.0
^{29}Ne$(3/2^-_2) \otimes n(p_{3/2})$	4.4	4.1
^{29}Ne$(7/2^-_1) \otimes n(f_{7/2})$	36.6	17.9
^{29}Ne$(1/2^+_1) \otimes n(s_{1/2})$	9.3	35.6
^{29}Ne$(1/2^+_2) \otimes n(s_{1/2})$	39.1	3.7
^{29}Ne$(5/2^+_1) \otimes n(d_{5/2})$	0.3	2.7
Inclusive (below 0.963 MeV)	94.0	112.9

4. Conclusions

In summary, single-proton (-neutron) cross sections were measured for ^{30}Ne with large $|\Delta S|$ at incident energies around 230 MeV/nucleon. The one-proton (-neutron) removal cross section producing ^{29}F (^{29}Ne) was calculated by ERT with the g.s. configuration and the spectroscopic factor predicted by the SM or AMD. In the models, g.s. spin-parity values of $5/2^+$ and $3/2^+$ were calculated for ^{29}F and ^{29}Ne. For the one-proton removal process, theoretical analysis confirmed that the measured cross section for the g.s. of ^{29}F was free from contaminations of low-lying states. On the other hand, for the one-neutron removal process, no clear conclusion on the contamination was drawn because of the quite dense energy levels of ^{29}Ne predicted by the two models. The experimental inclusive cross sections are compared to the calculations $R_s = \sigma(\text{expt})/\sigma(\text{theory})$. The R_s values are obtained with the spectroscopic factors given by the SM or AMD, respectively. The asymmetry dependence of R_s values deduced using SM is two times larger than that deduced using AMD. The discrepancy in R_s deduced using SM for the deeply bound nucleon removal reaction is consistent with the systematics observed from the knockout reactions at incident energies $\sim$ 100 MeV/nucleon. Together with the present one-proton removal of ^{30}Ne at $\sim$ 230 MeV/u, the same measurement at $\sim$ 100 MeV/u would be desirable for studying the energy dependence in the reaction model without additional uncertainties attributed to the structure input. For loosely bound nucleon removal, the present work gives a significantly smaller R_s for ^{29}Ne than the established systematics of R_s, which is close to unity. Such deviation might suggest the need for further improvement in the SM and AMD calculations for the structures of ^{30}Ne and ^{29}Ne.

Acknowledgements

The authors express their gratitude to the RIBF accelerator staff and the BigRIPS team for their contribution to the experiment.

References

[1] W. H. Dickhoff and D. V. Neck, *Many-body Theory Exposed* (World Scientific, Singapore, 2008).
[2] V. R. Pandharipande, I. Sick, and P. K. A. deWitt Huberts, Rev. Mod. Phys. **69**, 981 (1997).
[3] W. H. Dickoff and C. Barbieri, Prog. Part. Nucl. Phys. **52**, 377 (2004).
[4] A. Gade et al., Phys. Rev. C **77**, 044306 (2008) and references therein.
[5] J. Lee et al., Phys. Rev. Lett. **104**, 112701 (2010).
[6] J. Lee et al., Phys. Rev. C **83**, 014606 (2011).
[7] M. B. Tsang et al., Phys. Rev. Lett. **95**, 222501(2005).
[8] J. Lee et al., Phys. Rev. C **73**, 044608 (2006).
[9] J. Lee et al., Phys. Rev. C **75**, 064320 (2007).
[10] M. B. Tsang et al., Phys. Rev. Lett. **102**, 062501 (2009).
[11] R. J. Charity et al., Phys. Rev. Lett. **97**, 162503 (2006).
[12] R. J. Charity et al., Phys. Rev. C **76**, 044314 (2007).
[13] C. Barbieri, Phys. Rev. Lett. **103**, 202502 (2009).
[14] Ø. Jensen et al., Phys. Rev. Lett. **107**, 032501 (2011).
[15] F. Flavigny et al., Phys. Rev. Lett. **110**, 122503 (2013).
[16] F. Flavigny et al., Phys. Rev. Lett. **108**, 252501 (2012).
[17] J. A. Tostevin et al., J. Phys. G: Nucl. Part. Phys. **25**, 735 (1999).
[18] P. G. Hansen and J. A. Tostevin, Annu. Rev. Nucl. Part. Sci. **53**, 221 (2003).
[19] P. E. Hodgson, *Nuclear Heavy Ion Reaction* (Clarendon, Oxford, UK, 1978).
[20] G. F. Grinyer et al., Phys. Rev. C **86**, 024315 (2012).
[21] Y. Yano, Nucl. Instrum. Meth. B **261**, 1009 (2007).
[22] T. Kubo et al., Prog. Theor. Exp. Phys. **2012**, 03C003 (2012).
[23] S. Takeuchi et al., Nucl. Instrum. Meth. A **763**, 596 (2014).
[24] Y. Utsuno et al., Phys. Rev. C **60**, 054315 (1999).
[25] J. F. Berger, M. Girod, and D. Gogny, Comput. Phys. Commun. **63**, 365 (1991).
[26] M. Kimura, Phys. Rev. C **75**, 041302 (2007).
[27] T. Sumi et al., Phys. Rev. C **85**, 064613 (2012).
[28] S. Watanabe et al., Phys. Rev. C **89**, 044610 (2014).
[29] V. Tripathi et al., Phys. Rev. Lett. **94**, 162501 (2005).
[30] A. M. Hurst et al., Phys. Lett. B **674**, 168 (2009).
[31] V. Tripathi et al., Phys. Rev. Lett. **101**, 142504 (2008).
[32] V. Tripathi et al., Phys. Rev. Lett. **104**, 129202 (2010).
[33] D. T. Yordanov et al., Phys. Rev. Lett. **104**, 129201 (2010).
[34] K. Minomo et al., Phys. Rev. Lett. **108**, 052503 (2012).
[35] M. Takechi et al., Mod. Phys. Lett. A **25**, 1878 (2010).
[36] N. Kobayashi et al., Phys. Rev. C **93**, 014613 (2016).
[37] M. Yahiro, K. Ogata, and K. Minomo, Prog. Theor. Phys. **126**, 167 (2011).
[38] K. Minomo et al., Phys. Rev. C **90**, 027601 (2014).
[39] M. Yahiro et al., Prog. Theor. Exp. Phys. **2012**, 01A206 (2012).
[40] J. A. Tostevin and A. Gade, Phys. Rev. C **90**, 057602 (2014).
[41] L. Gaudefroy et al., Phys. Rev. Lett. **109**, 202503 (2012).
[42] M. Wang et al., Chinese Physics C **36**, 1603 (2012).